

Cardiac Magnetic Resonance Imaging

Delayed Contrast-Enhanced Magnetic Resonance Imaging for the Prediction of Regional Functional Improvement After Acute Myocardial Infarction

Aernout M. Beek, MD,* Harald P. Kühl, MD,* Olga Bondarenko, MD,* Jos W. R. Twisk, PhD,†
Mark B. M. Hofman, PhD,‡ Willem G. van Dookum, MD,* Cees A. Visser, MD, PhD,*
Albert C. van Rossum, MD, PhD*

Amsterdam, The Netherlands

OBJECTIVES	We evaluated whether delayed contrast-enhanced magnetic resonance imaging (DCE-MRI) using an extracellular contrast agent could predict improvement of dysfunctional but viable myocardium after acute reperfused myocardial infarction (MI).
BACKGROUND	The transmural extent of hyperenhancement at DCE-MRI has been related to improvement of function in reperfused MI. However, evidence is still limited, and earlier reports have produced conflicting results regarding the significance of contrast patterns after infarction.
METHODS	Thirty patients (mean age 59 ± 11 years, 27 males) underwent cine MRI and DCE-MRI 7 ± 3 days after a first reperfused acute MI and follow-up cine MRI at 13 ± 3 weeks. Segmental wall thickening and segmental extent of hyperenhancement were scored in 1,689 segments.
RESULTS	Of 500 dysfunctional segments, 273 (55%) improved at follow-up. There was no difference in likelihood of improvement or complete functional recovery between segments with 0% and 1% to 25% hyperenhancement. The likelihood of improvement of segments without hyperenhancement was 2.9, 14.3, and 20 times higher than that of segments with 26% to 50%, 51% to 75%, and >75% hyperenhancement, respectively ($p < 0.001$). The likelihood of complete functional recovery of segments without hyperenhancement was 3.8, 11.1, and 50 times higher than that of segments with 26% to 50%, 51% to 75%, and >75% hyperenhancement, respectively ($p < 0.001$).
CONCLUSIONS	In patients with recent reperfused MI, functional improvement of stunned myocardium is predicted by DCE-MRI. (J Am Coll Cardiol 2003;42:895-901) © 2003 by the American College of Cardiology Foundation

The recognition of stunned myocardium early after acute myocardial infarction (AMI) has important prognostic and therapeutic implications (1). Using low-dose dobutamine echocardiography and ^{18}F -fluorodeoxyglucose-positron emission tomography, a subgroup of patients with residual myocardial viability has been identified that is at high risk

See page 902

for future clinical events (2,3). Contrast-enhanced magnetic resonance imaging (MRI) using an extracellular contrast agent such as gadolinium-diethylenetriamine pentaacetic acid (Gd-DTPA) has been applied extensively for the evaluation of myocardial injury after AMI (4-11). In a recent series of studies using canine infarction models, it has been shown that hyperenhancement on T1-weighted delayed contrast-enhanced magnetic resonance imaging

(DCE-MRI) (originally described as images acquired more than 10 min after contrast injection) only occurred in necrotic, irreversibly injured myocardium, irrespective of the age of the infarct (12,13). The high signal intensity is related to a regional increased concentration of the contrast agent, most likely caused by ischemia-related changes in the volume of distribution and contrast kinetics (14-16). The regional extent of hyperenhancement has been shown to predict functional improvement of stunned myocardium, both in a canine model and recently also in patients with reperfused myocardial infarction (MI) (10,11,17). However, evidence is still limited, and earlier reports have produced conflicting results on the significance of contrast patterns after MI. Several investigators have demonstrated that the hyperenhanced region overestimates the actual necrotic region, and that it contains residual viable myocardium that may recover function when adequately reperfused (8,18,19). Comparison between these studies is hampered by considerable methodological differences, including the MRI technique that was used, the contrast dose, and the clinical or experimental setting. The current standard DCE-MRI technique combines optimal image quality, high spatial resolution, and contrast-to-noise and is a promising tool for the transmural evaluation of myocardial viability (10,11,20).

From the Departments of *Cardiology, †Clinical Epidemiology and Biostatistics, and ‡Clinical Physics and Informatics, Vrije Universiteit Medical Center, Amsterdam, The Netherlands. This study was supported by the Netherlands Heart Foundation (O.B., grant 2001.158) and the Interuniversity Cardiology Institute of the Netherlands.

Manuscript received August 27, 2002; revised manuscript received February 17, 2003, accepted March 7, 2003.

Abbreviations and Acronyms

AMI	= acute myocardial infarction
CK	= creatine kinase
DCE	= delayed contrast-enhanced
DTPA	= diethylenetriamine pentaacetic acid
ECG	= electrocardiogram
EF	= ejection fraction
MI	= myocardial infarction
MRI	= magnetic resonance imaging
PTCA	= percutaneous transluminal coronary angioplasty
SEH	= segmental extent of hyperenhancement
SEH _{th}	= SEH scored after thresholding the window setting of contrast images
SWT	= segmental wall thickening
TI	= inversion time

We therefore conducted a prospective study to evaluate the role of this DCE-MRI technique in the prediction of functional improvement in patients with first AMI.

METHODS

Patient population. Patients were eligible for the study if admitted with first AMI according to standard electrocardiogram (ECG) and enzymatic criteria. Only patients with direct (coronary catheterization, Thrombolysis In Myocardial Infarction flow grade 3 in the infarct-related artery) or indirect (rapid decrease of symptoms and more than 50% resolution of ST elevation on ECG, either during or after thrombolytic therapy or spontaneous) evidence of successful reperfusion were included. Exclusion criteria were hemodynamic instability, failure to give informed consent, or any relative or absolute contraindication for MRI. The study is part of a larger project evaluating the current role of contrast-enhanced MRI in patients with suspected ischemic heart disease, which was approved by the Committee on Research Involving Human Subjects of the Vrije Universiteit Medical Center. Thirty-nine patients were initially enrolled. Nine patients were excluded from the final analysis: one patient had significant valvular disease, four patients were lost to follow-up, and four patients had insufficient image quality of either baseline or follow-up MRI study. The clinical characteristics of the remaining 30 patients are listed in Table 1. Five patients (4 spontaneous symptom and ECG resolution, 1 thrombolysis) were revascularized between the baseline and follow-up MRI study. In three of these, percutaneous transluminal coronary angioplasty (PTCA) of the infarct-related artery was performed before discharge because of symptomatic ischemia during exercise testing. Two patients were readmitted with unstable angina pectoris with negative cardiac enzymes and underwent PTCA (of the infarct-related artery) and coronary artery bypass graft surgery, respectively.

MRI. All MRI procedures were performed with the patient in supine position in a 1.5-T clinical scanner (Sonata/Vision, Siemens, Erlangen, Germany) using a four-element phased array cardiac receiver coil. The ECG-gated images

Table 1. Patient Characteristics

Number of patients	30
Male	28
Age (yrs)	59 ± 11
Infarct site ECG	
Anterior	13
Inferior (lateral)	11
Posterior	6
Maximum total CK (U/l)	2,190 ± 1,364
Maximum MB fraction	178 ± 110
Ejection fraction baseline (%)	51 ± 9
Thrombolysis	5
Primary PTCA	8
Days between admission and baseline MRI	7 ± 3
Weeks between admission and follow-up MRI	13 ± 3

CK = creatine kinase; ECG = electrocardiogram; MRI = magnetic resonance imaging; PTCA = percutaneous coronary transluminal angioplasty.

were acquired during repeated breath-holds of varying duration depending on heart rate (~10 s). Cine images using a segmented gradient-echo sequence (6-mm slice thickness) were obtained in multiple short-axis views every 10 mm covering the whole left ventricle (LV). Ten to 15 min after injection of a gadolinium-based contrast agent (Magnevist, Schering AG, Berlin, Germany; 0.2 mmol/kg), DCE images were acquired in the same orientation as the cine images using a segmented inversion-recovery gradient-echo pulse sequence (repetition time/echo time = 9.6/4.4 ms, flip angle 25°, matrix 208 × 256 and a typical voxel size of 1.6 × 1.3 × 5.0 mm, inversion time [TI] 250 to 300 ms). The baseline study was performed 7 ± 3 days after admission, with follow-up at 13 ± 3 weeks. The DCE images were acquired only during the baseline study.

Data analysis. All data were analyzed on a separate workstation (Sun Microsystems, Inc., Santa Clara, California) using a dedicated software package (Mass, Medis, Leiden, The Netherlands). Baseline cine images and contrast-enhanced images were matched by using slice position, because both data sets were acquired during the same imaging session. Registration of follow-up to baseline cine images was achieved by consensus of two observers using various anatomic landmarks, including the septal insertion sites of the right ventricle, the papillary muscles, and trabecularization patterns in the right ventricle and LV. Images were then analyzed by consensus of two observers who were blinded to patient data and the results of the other examinations.

Segmental analysis. For analysis of segmental function and contrast pattern, the two most basal and two most distal slices were excluded, because short-axis images at these levels preclude a reliable segmental evaluation owing to the presence of the LV outflow tract and small diameter, respectively. Each short axis was divided in 12 equi-angular segments, starting at the posterior septal insertion of the right ventricle. Segmental wall thickening (SWT) was scored according to the following scale: 1—normal, 2—mild hypokinesis, 3—severe hypokinesis, 4—akinesis, 5—dyskinesis. Functional improvement was defined as a decrease in SWT score of ≥1. Complete recovery was defined as a

decrease to SWT score 1. Interobserver variability (A.M.B., H.P.K.) was tested in 10 patients (532 segments).

For analysis of the DCE images, the segmental extent of hyperenhancement (SEH) was calculated by dividing the hyperenhanced area by the total area of the predefined segment expressed as percentage. Any subendocardial area of hypoenhancement within the hyperenhanced area was considered part of the hyperenhanced area. The SEH was then scored as follows: 1—0%; 2—1% to 25%; 3—26% to 50%; 4—51% to 75%; 5—76% to 100% hyperenhancement (10). To explore the relationship between DCE-MRI and change in ejection fraction (EF), we calculated a viability score in each patient as follows: the total number of segments with baseline wall thickening abnormality and SEH score ≤ 2 , divided by all segments with baseline wall thickening abnormality.

The assessment of contrast images and the size of the hyperenhanced areas are sensitive to image window setting. To eliminate the influence of subjective window setting, SEH was scored again after thresholding the images at 6 SD above signal intensity of the opposite, non-infarcted myocardium in the same slice (SEH_{th}). The choice of 6 SD as the cutoff value was based on our own clinical experience and recent literature (21). To test the interobserver variability (A.M.B., O.B.), SEH was scored independently in five patients (299 segments), with window setting adjusted to personal preference.

Global analysis. On all short-axis cine slices, the endocardial and epicardial borders were outlined manually in end-diastolic and end-systolic images, excluding trabeculae and papillary muscles. The EF was calculated as follows: (end-diastolic volume - end-systolic volume)/end-diastolic volume.

Statistical analysis. The paired sample *t* test and the independent samples *t* test were used to compare means within the study group or between subgroups. We used kappa values to assess interobserver variability and enhancement score (SEH and SEH_{th}) variability. Because wall thickening scores within one patient are strongly related, we used multilevel logistic regression to evaluate the relationship between change in wall thickening and baseline hyperenhancement score (MLwiN, version 1.02.0002, Centre for Multilevel Modelling, London, United Kingdom) (22,23). Multilevel analysis can be considered an extension to the commonly used repeated measures analysis of variance, which has the disadvantage that only a continuous outcome variable can be analyzed. Furthermore, repeated measures analysis of variance requires a fully balanced data set and only corrects for correlated observations at one level. In this study, two dichotomous outcome variables were analyzed (improvement and complete recovery), with correlated observations at two levels (i.e., slices within patients and segments within slices). A correction was made for baseline wall thickening scores, and the regression equation was used to calculate odds ratios that expressed the likelihood of improvement relative to functional outcome of segments without hyperenhancement (SEH score 1). The relationship between change in EF and various patient variables was evaluated using logistic regression.

RESULTS

A total of 1,740 segments (4.8 slices/patient) were available for analysis. During the analysis, 51 (3%) segments were additionally excluded because assessment was considered not reliable on any of the cine or contrast images by at least one of the two observers (e.g., presence of LV outflow tract, localized artifacts).

Cine MRI. Of 1,689 segments, 500 (30%) showed a baseline wall thickening abnormality. In these, baseline mean SWT score was 3.2 ± 0.9 . At follow-up, mean SWT score had decreased to 2.5 ± 1.3 ($p < 0.001$ vs. baseline). Fifty-five percent (273 of 500) of segments improved at follow-up, 7% (36 segments) worsened, and 38% (191 segments) remained unchanged. Interobserver agreement for the assessment of SWT was 85% (kappa = 0.69).

DCE-MRI. Twenty-nine patients showed regional hyperenhancement, and in all patients the area corresponded to the electrocardiographic infarct location. One patient with a small inferior infarction (maximum creatine kinase [CK] = 426 U/l) had no regional hyperenhancement. The interobserver agreement for the assessment of SEH was 87% (kappa = 0.76).

Segments that improved had lower mean SEH score than segments that did not improve (2.4 ± 1.3 vs. 3.7 ± 1.4 ; $p < 0.001$). The functional change according to SEH is shown in Figure 1A and Table 2. Of 151 segments with $\leq 25\%$ hyperenhancement that improved, 119 (79%) had complete functional recovery, 25 (17%) residual mild hypokinesis, and 7 (5%) residual severe hypokinesis. Of the 31 segments with $> 75\%$ hyperenhancement that improved, only 4 (13%) had complete functional recovery, 9 (29%) residual mild hypokinesis, and 17 (55%) initially akinetic segments and one initially dyskinetic segment had residual severe hypokinesis. Figure 2 illustrates the relationship between hyperenhancement and change in wall thickening in a patient with recent anterior MI (also see electronic data supplement at www.cardiosource.com/jacc.html, September 3 JACC issue).

Multilevel analysis showed that the inverse relationship between likelihood of improvement and SEH was highly significant. Functional outcome in relation to contrast score is shown in Table 3. The outcome was comparable in segments with SEH scores 1 and 2. The likelihood of partial or complete functional recovery of segments without hyperenhancement (SEH score 1) was significantly higher than that of segments with SEH scores 3, 4, and 5. Segments without hyperenhancement were 20 and 50 times more likely to have partial or complete recovery of function, respectively, than segments with $> 75\%$ hyperenhancement (Table 3).

ANALYSIS USING STANDARDIZED WINDOW SETTING (SEH_{th}). The overall agreement between the SEH score and the SEH_{th} score was 85% (kappa = 0.70). Agreement was lower when only the 500 segments with abnormal baseline wall thickening were taken into account: 64% (SEH $<$ SEH_{th} in 24% of segments, SEH $>$ SEH_{th} in 12% of segments) (kappa = 0.55). The functional change according

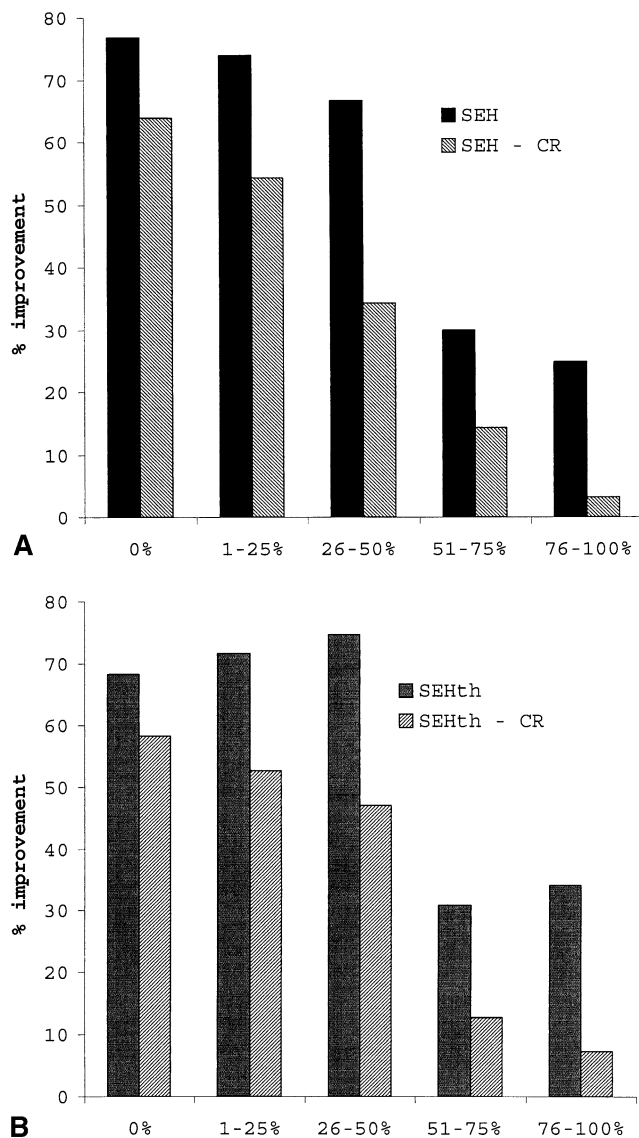


Figure 1. Functional outcome of dysfunctional segments according to baseline segmental extent of hyperenhancement (A = SEH; B = SEH_{th}). CR = complete recovery. Also see Table 2.

to baseline SEH_{th} is shown in Figure 1B and Table 2. Multilevel analysis showed that the likelihood of partial or complete functional recovery was similar for SEH_{th} scores 1, 2, and 3 and was significantly lower for SEH_{th} scores 4 and 5 (Table 3).

SUBENDOCARDIAL DARK ZONE. Sixty-five segments had a subendocardial zone of low signal intensity within the hyperenhanced region. Mean wall thickening score at baseline in these segments was high (3.8 ± 0.5) and remained high at follow-up (3.8 ± 0.6 ; $p = \text{NS}$). Only 10 of these (15%) showed improvement: 6 initially akinetic segments had residual severe hypokinesis, 3 akinetic segments had residual mild hypokinesis, and only 1 segment had complete recovery. Of the remaining 55 segments, 45 remained akinetic, 1 remained severely hypokinetic, and 9 worsened.

LVEF. Overall EF did not change at follow-up (0.51 ± 0.09 vs. 0.53 ± 0.10 , $p = \text{NS}$). Previous studies have reported a significant relationship between the percentage dysfunctional but viable myocardium and the change in EF (10,21). We tested multiple patient-related and scan-related variables for their ability to predict the change in EF at follow-up: age; baseline EF; maximum CK; maximum CK, MB fraction; the presence of a dark zone; and the viability score. No significant predictors of change in EF could be identified (Table 4). However, the study group was small, and some variables (the viability score, presence of a dark zone) might have reached statistical significance with a larger study group size.

DISCUSSION

This study shows that DCE-MRI can be used to predict improvement of dysfunctional but viable myocardium in patients with recent reperfused MI. The likelihood of functional improvement decreased with increasing SEH. Multilevel logistic regression analysis, which takes into account the fact that segments within one patient and one slice are strongly correlated, showed that this inverse relationship was highly significant.

Hyperenhancement after recent MI. High-resolution experimental studies that used the current standard DCE-MRI technique have demonstrated that hyperenhanced areas correlate exclusively with irreversibly damaged, necrotic myocardium at various time intervals after infarction and irrespective of the status of the infarct-related artery (12,13). Hillenbrand et al. (17) used a canine infarction model to evaluate functional recovery after various occlusion times and found that both likelihood of improvement and change in absolute wall thickening were predicted by the transmural extent of hyperenhancement. Using electron probe X-ray microanalysis, Rehwald et al. (16) showed that elevations in Gd-DTPA concentration only occur in regions with histologically proven irreversible ischemic damage. Our data are in line with these experimental and two recent clinical studies that used the same MRI technique to evaluate viability after recent MI. Choi et al. (10) studied 24 patients one week and 16 ± 6 weeks after infarction and found that the transmural extent of hyperenhancement strongly predicted functional improvement. Gerber et al. (11) evaluated 20 patients with contrast-enhanced MRI and myocardial tagging and found that improvement in circumferential shortening was inversely related to the regional extent of hyperenhancement at delayed imaging. Compared with Choi et al. (10), we found that more segments with >75% hyperenhancement improved at follow-up (25% [31 of 125] vs. 5% [3 of 64]), although the majority of these segments had severe residual dysfunction and only four had complete recovery. Gerber et al. (11) reported the mean functional improvement but did not state the percentage of segments with >75% hyperenhancement that improved. Hillenbrand et al. (17) also found some improvement (12%)

Table 2. Number of Segments With Functional Improvement and CR at Follow-Up According to Baseline SEH- and SEH_{th}-score*

SEH					
Total	108	92	105	70	125
Improved	83	68	70	21	31
CR	69	50	36	10	4
SEH _{th}					
Total	120	74	87	55	164
Improved	82	53	65	17	56
CR	70	39	41	7	12
SEH/SEH _{th} -score	1	2	3	4	5

*Also see Figure 2.

CR = complete recovery; SEH = segmental extent of hyperenhancement; SEH_{th} = SEH scored after thresholding the images at 6 SD above signal intensity of the opposite, non-infarcted myocardium in the same slice.

in segments with extensive enhancement in their canine experiment. Results of the highly detailed experimental studies make it unlikely that Gd-DTPA accumulates in reversibly damaged myocardium, although one cannot entirely exclude the possibility that distribution of Gd-DTPA in human and canine infarcts is different. However, several other factors may have played a role.

An important issue and potential source of error was recently evaluated by Oshinski *et al.* (24), who found that MRI overestimated infarct size in a rat model of reperfused infarction when images were acquired too early after contrast injection. However, these authors used a different pulse sequence (single slice spin-echo sequence with an acquisition time of 2 to 3 min) with a fixed TI and a different contrast dose (0.03 mmol/kg), which interferes with extrapolation of their results to our study (25). In the literature, the time between contrast injection and data acquisition varies considerably, between 5 and 30 min (8,12,13,17, 18,20). In our study, DCE-MRI data acquisition was

started 10 to 15 min after contrast injection, and we did not notice a decrease in hyperenhanced area over time. However, we did not systematically evaluate time dependency of size of infarction, and future study is required.

Another possible cause of error is related to the use of qualitative assessment of regional wall thickening. Tethering of largely non-viable segments to surrounding viable segments regaining contraction may falsely give the impression of improved function (17). In segments with >75% hyperenhancement, the likelihood of improvement was twice the likelihood of complete recovery, which suggests that it may be more difficult to establish partial recovery with severe residual dysfunction than complete recovery. In addition, all studies that use the change in regional wall thickening as the standard of viability require accurate registration of baseline and follow-up images. Despite the use of standard imaging procedures and anatomic landmarks, misregistration may be caused by infarct sequelae as scar formation and remodeling.

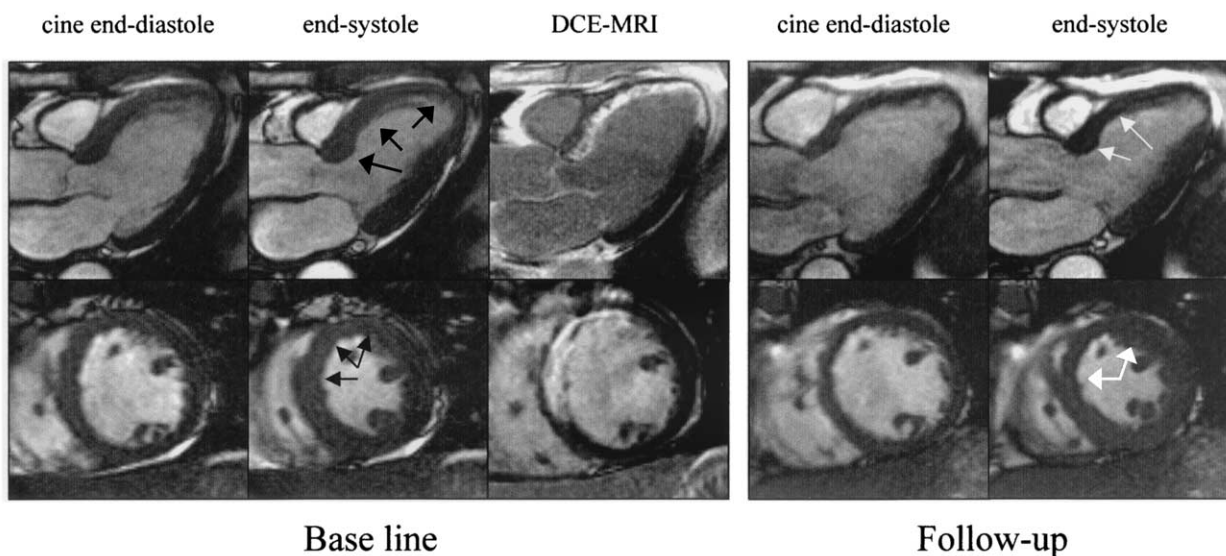


Figure 2. Three-chamber view and short axis view in a patient 5 days and 12 weeks after primary percutaneous transluminal coronary angioplasty plus stenting of the left anterior descending coronary artery for anterior myocardial infarction. Baseline cine (**left**) shows severe wall thickening abnormality (**black arrows**) in the anteroseptal, anterior, and apical region. Follow-up cine (**right**) shows no improvement in the area with transmural hyperenhancement, whereas some improvement can be seen in the areas with non-transmural hyperenhancement (**white arrows**). To view cines in motion, please see the accompanying videos corresponding to Figure 2 (Videos 1, 2, 3, and 4) at www.cardiosource.com/jacc.html (see September 3 *JACC* issue).

Table 3. Multilevel Logistic Regression Analysis*

		Improvement		Complete Recovery	
		OR	p	OR	p
SEH score	2	0.63 (0.26–1.55)	0.32	0.81 (0.36–1.82)	0.61
	3	0.35 (0.14–0.88)	0.03	0.26 (0.11–0.59)	0.00
	4	0.07 (0.03–0.20)	0.00	0.09 (0.03–0.26)	0.00
	5	0.05 (0.02–0.13)	0.00	0.02 (0.01–0.11)	0.00
SEH _{th} score	2	0.66 (0.26–1.55)	0.32	0.70 (0.31–1.61)	0.41
	3	0.79 (0.34–1.86)	0.59	0.52 (0.22–1.23)	0.14
	4	0.12 (0.04–0.34)	0.00	0.10 (0.03–0.37)	0.00
	5	0.09 (0.04–0.23)	0.00	0.03 (0.01–0.11)	0.00

*Odds ratios (95% confidence interval) represent likelihood of improvement or recovery relative to outcome of segments with SEH and SEH_{th} score 1.

Odds ratio (OR) = EXP (regression coefficient). Other abbreviations as in Table 2.

Definition of hyperenhancement—current limitations of DCE-MRI. During data acquisition, the area of hyperenhancement is defined by suppressing the signal of remote myocardium without elevated Gd-DTPA concentrations. Therefore, DCE-MRI may be less reliable when there is coexisting myocardial disease with diffuse or regional fibrosis. In addition, careful optimization and continuous adjustment of the TI is required, because ongoing wash-out of contrast in remote, non-infarcted myocardium causes continuous change of myocardial relaxation parameters (20). Currently, the correct choice of TI largely depends on the experience of the operator, making it a potential source of error. Newer reconstruction methods that are more operator-independent are being developed (26).

During image analysis, the definition of hyperenhancement is not standardized. Signal intensities and area of enhancement are influenced by window setting, which may inappropriately define segmental viability status. Animal studies have used objective thresholds related to the nulled signal of remote, non-enhanced myocardium, defining “hyperenhanced” as more than 2 or 3 SD above the mean signal intensity of remote (12,13,17,27). Studies in patients have generally not reported the use of objective definitions of hypoenhancement and hyperenhancement (8,10,18,28). In our experience, thresholding the images at 2 or 3 SD above remote grossly overestimates the visually determined areas. Signal intensity of remote myocardium is actively suppressed and is therefore so low that areas that have only marginally higher signal intensity are falsely considered part of the infarcted area. In a group of patients with chronic

ischemic heart disease, Kim et al. (21) reported that signal intensity in regions of interest within the hyperenhanced infarcted area was always more than 6 SD above non-enhanced remote regions, although this was not used in the actual analysis. In the subset of segments with baseline abnormal wall thickening, we found that SEH_{th} scores correlated only moderately with the SEH scores (agreement 64%, overestimating in 24%, kappa 0.55). Multilevel analysis showed that the discriminative power of SEH_{th} was smaller than that of SEH, because only SEH_{th} scores 4 and 5 had significantly lower likelihood of improvement than SEH_{th} score 1. In addition, we found that on some occasions the presence of a dark zone could only be recognized on the non-thresholded images. The interobserver agreement between two observers who independently drew myocardial contours and adjusted window setting for non-thresholded SEH in our study was good (87%, kappa = 0.76).

Hypoenhancement at delayed imaging. Low signal intensity (hypoenhancement) during the first 2 min after contrast injection is attributed to microvascular obstruction (7,15). It is associated with greater myocardial damage and identifies patients with worse prognosis (7,28,29). Signal intensity in these dark zones rises slowly in the first 5 to 10 min after contrast injection (7,15). The extent of hypoenhancement may vary with the time after injection, because it is unlikely that the degree of microvascular damage is identical throughout the entire infarct. Some areas may have mild damage and allow slow contrast wash-in by diffusion from surrounding regions with intact microcirculation (Fig. 3) (30). Others may have extensive microvascular damage, resulting in persistent hypoenhancement even at late imaging. We found that segments with dark zones within the hyperenhanced areas at delayed imaging had poor function with very low likelihood of improvement at follow-up.

In conclusion, this study shows that DCE-MRI can be used to predict improvement of dysfunctional but viable segments in patients with recent reperfused MI. Future study should focus on further standardization of scan procedures and image analysis.

Table 4. Logistic Regression Analysis for the Prediction of the Change in Ejection Fraction

	Odds Ratio	95% CI	P
Age	1.00	0.93–1.08	0.93
CK	0.86	0.44–1.68	0.65
MB fraction	1.15	0.44–3.00	0.77
Presence of dark zone	2.40	0.48–12.13	0.29
Viability score (SEH ≤ 2)	1.40	0.95–2.07	0.10

CI = confidence interval; CK = creatine kinase; SEH = segmental extent of hyperenhancement.

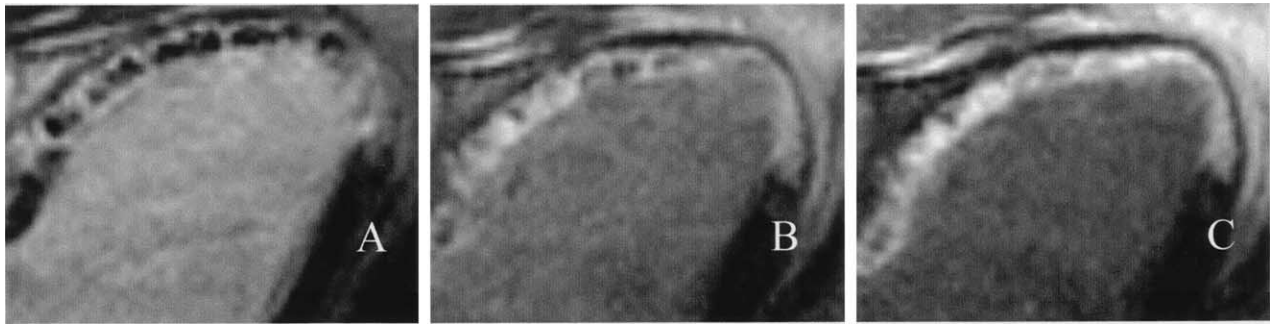


Figure 3. Temporal changes in signal intensity after 0.2 mmol/kg gadolinium-DTPA administered intravenously in the same patient as Figure 2. Magnified view of three-chamber view at 2 min (A), 15 min (B), and 30 min (C).

Reprint requests and correspondence: Dr. Aernout M. Beek, Department of Cardiology, VU Medical Center, De Boelelaan 1117, Amsterdam 1007 MB, The Netherlands. E-mail: am.beek@vumc.nl.

REFERENCES

1. Lee KS, Marwick TH, Cook SA, et al. Prognosis of patients with left ventricular dysfunction, with and without viable myocardium after myocardial infarction: relative efficacy of medical therapy and revascularization. *Circulation* 1994;90:2687-94.
2. Smart S, Wynsen J, Sagar K. Dobutamine-atropine stress echocardiography for reversible dysfunction during the first week after acute myocardial infarction: limitations and determinants of accuracy. *J Am Coll Cardiol* 1997;30:1669-78.
3. Schwaiger M, Brunken R, Grover-McKay M, et al. Regional myocardial metabolism in patients with acute myocardial infarction assessed by positron emission tomography. *J Am Coll Cardiol* 1986;8:800-8.
4. De Roos A, Van Rossum AC, van der Wall EE, et al. Reperfused and nonreperfused myocardial infarction: diagnostic potential of Gd-DTPA-enhanced MR imaging. *Radiology* 1989;172:717-20.
5. Van Rossum AC, Visser FC, Van Eenige MJ, et al. Value of gadolinium-diethylene-triamine pentaacetic acid dynamics in magnetic resonance imaging of acute myocardial infarction with occluded and reperfused coronary arteries after thrombolysis. *Am J Cardiol* 1990;65:845-51.
6. van der Wall EE, van Dijkman PR, De Roos A, et al. Diagnostic significance of gadolinium-DTPA (diethylenetriamine penta-acetic acid) enhanced magnetic resonance imaging in thrombolytic treatment for acute myocardial infarction: its potential in assessing reperfusion. *Br Heart J* 1990;63:12-7.
7. Lima JA, Judd RM, Bazille A, Schulman SP, Atalar E, Zerhouni EA. Regional heterogeneity of human myocardial infarcts demonstrated by contrast-enhanced MRI: potential mechanisms. *Circulation* 1995;92:1117-25.
8. Rogers WJJ, Kramer CM, Geskin G, et al. Early contrast-enhanced MRI predicts late functional recovery after reperfused myocardial infarction. *Circulation* 1999;99:744-50.
9. Dendale P, Franken PR, Block P, Pratikakis Y, De Roos A. Contrast enhanced and functional magnetic resonance imaging for the detection of viable myocardium after infarction. *Am Heart J* 1998;135:875-80.
10. Choi KM, Kim RJ, Gubernikoff G, Vargas JD, Parker M, Judd RM. Transmural extent of acute myocardial infarction predicts long-term improvement in contractile function. *Circulation* 2001;104:1101-7.
11. Gerber BL, Garot J, Bluemke DA, Wu KC, Lima JA. Accuracy of contrast-enhanced magnetic resonance imaging in predicting improvement of regional myocardial function in patients after acute myocardial infarction. *Circulation* 2002;106:1083-9.
12. Kim RJ, Fieno DS, Parrish TB, et al. Relationship of MRI delayed contrast enhancement to irreversible injury, infarct age, and contractile function. *Circulation* 1999;100:1992-2002.
13. Fieno DS, Kim RJ, Chen EL, Lomasney JW, Klocke FJ, Judd RM. Contrast-enhanced magnetic resonance imaging of myocardium at risk: distinction between reversible and irreversible injury throughout infarct healing. *J Am Coll Cardiol* 2000;36:1985-91.
14. Kim RJ, Chen EL, Lima JA, Judd RM. Myocardial Gd-DTPA kinetics determine MRI contrast enhancement and reflect the extent and severity of myocardial injury after acute reperfused infarction. *Circulation* 1996;94:3318-26.
15. Judd RM, Lugo-Olivieri CH, Arai M, et al. Physiological basis of myocardial contrast enhancement in fast magnetic resonance images of 2-day-old reperfused canine infarcts. *Circulation* 1995;92:1902-10.
16. Rehwald WG, Fieno DS, Chen EL, Kim RJ, Judd RM. Myocardial magnetic resonance imaging contrast agent concentrations after reversible and irreversible ischemic injury. *Circulation* 2002;105:224-9.
17. Hillenbrand HB, Kim RJ, Parker MA, Fieno DS, Judd RM. Early assessment of myocardial salvage by contrast-enhanced magnetic resonance imaging. *Circulation* 2000;102:1678-83.
18. Kramer CM, Rogers WJ Jr., Mankad S, Theobald TM, Pakstis DL, Hu YL. Contractile reserve and contrast uptake pattern by magnetic resonance imaging and functional recovery after reperfused myocardial infarction. *J Am Coll Cardiol* 2000;36:1835-40.
19. Saeed M, Lund G, Wendland MF, Bremerich J, Weinmann H, Higgins CB. Magnetic resonance characterization of the peri-infarction zone of reperfused myocardial infarction with necrosis-specific and extracellular nonspecific contrast media. *Circulation* 2001;103:871-6.
20. Simonetti OP, Kim RJ, Fieno DS, et al. An improved MR imaging technique for the visualization of myocardial infarction. *Radiology* 2001;218:215-23.
21. Kim RJ, Wu E, Rafael A, et al. The use of contrast-enhanced magnetic resonance imaging to identify reversible myocardial dysfunction. *N Engl J Med* 2000;343:1445-53.
22. Goldstein H. *Multilevel Statistical Models*. London: Edward Arnold, 1995.
23. Goldstein H, Rashback J, Plewis I, et al. *A User's Guide to MLwiN*. London: Institute of Education, 1998.
24. Oshinski JN, Yang Z, Jones JR, Mata JF, French BA. Imaging time after Gd-DTPA injection is critical in using delayed enhancement to determine infarct size accurately with magnetic resonance imaging. *Circulation* 2001;104:2838-42.
25. Judd RM, Kim RJ. Imaging time after Gd-DTPA injection is critical in using delayed enhancement to determine infarct size accurately with magnetic resonance imaging (reply). *Circulation* 2002;106:e6.
26. Kellman P, Arai AE, McVeigh ER, Aletras AH. Phase-sensitive inversion recovery for detecting myocardial infarction using gadolinium-delayed hyperenhancement. *Magn Reson Med* 2002;47:372-83.
27. Gerber BL, Rochitte CE, Bluemke DA, et al. Relation between Gd-DTPA contrast enhancement and regional inotropic response in the periphery and center of myocardial infarction. *Circulation* 2001;104:998-1004.
28. Wu KC, Zerhouni EA, Judd RM, et al. Prognostic significance of microvascular obstruction by magnetic resonance imaging in patients with acute myocardial infarction. *Circulation* 1998;97:765-72.
29. Gerber BL, Rochitte CE, Melin JA, et al. Microvascular obstruction and left ventricular remodeling early after acute myocardial infarction. *Circulation* 2000;101:2734-41.
30. Mahrholdt H, Wagner A, Judd RM, Sechtem U. Assessment of myocardial viability by cardiovascular magnetic resonance imaging. *Eur Heart J* 2002;23:602-19.